

Surface vacancies at the fivefold icosahedral Al-Pd-Mn quasicrystal surface: A comparison of *ab initio* calculated and experimental STM images

M. Krajčí,^{1,2} J. Hafner,¹ J. Ledieu,^{3,4} and R. McGrath³

¹Institut für Materialphysik and Center for Computational Materials Science, Universität Wien, Sensengasse 8/12, A-1090 Wien, Austria

²Institute of Physics, Slovak Academy of Sciences, Dúbravská cesta 9, SK-84511 Bratislava, Slovak Republic

³Surface Science Research Centre and Department of Physics, The University of Liverpool, Liverpool L69 3BX, United Kingdom

⁴LSG2 M, CNRS UMR 7584, Ecole des Mines, Parc de Saurupt, 54042, Nancy Cedex, France

(Received 3 October 2005; published 10 January 2006)

Scanning tunneling microscopy (STM) images of the fivefold surface of the icosahedral (*i*) Al-Pd-Mn quasicrystal have been calculated using *ab initio* density functional methods. The STM signal is formed predominantly by the Al atoms in the surface plane. The Pd atoms are seen in the STM image as dark spots. The reason for their small contribution to the STM current is a small local density of states around the Fermi level and the localized *d*-character of the Pd states. On the other hand, the local paramagnetic density of states on Mn atoms is much higher than that on Pd atoms and therefore Mn atoms are seen in the STM images as bright spots. A direct comparison of the experimental images obtained from the STM with the *ab initio* calculated STM images reveals that the characteristic features of the images—the dark pentagonal holes—can also be created by surface vacancies and not only by truncated Bergman clusters as it has been supposed up to now.

DOI: [10.1103/PhysRevB.73.024202](https://doi.org/10.1103/PhysRevB.73.024202)

PACS number(s): 61.44.Br, 71.23.Ft, 68.37.Ef, 71.20.-b

I. INTRODUCTION

More than 20 years after the discovery of quasicrystals the description of their structure at an atomic scale remains a difficult subject. Although it is generally argued that the skeleton of the quasicrystalline structures can be reasonably well-described on the basis of cut-and-projection models from higher-dimensional space, the positions of the atoms and their local coordination depend on the details of the acceptance domains in perpendicular space which have only been determined using diffraction data in a small number of cases.¹ In certain favorable cases the precise atomic positions of the atoms can be inferred from the known crystal structures of low-order periodic approximants.

In principle scanning tunneling microscopy (STM) of quasicrystalline surfaces with atomic resolution could supply much of the missing information. However, STM does not image the atomic structure of a surface, but rather the electron density distribution in a certain energy interval below or above the Fermi level and at a certain distance above the surface, depending on the position of the tip of the scanning microscopy, the voltage between the tip and the sample, and the magnitude and polarity of the tunnel current. Experience with STM on complex crystalline surfaces has taught the lesson that hand-weaving interpretations can be quite misleading. On the other hand, it has been demonstrated that STM experiments combined with *ab initio* electronic structure calculations represent an extremely powerful tool for the structure analysis of even very complex systems—a recent example is the analysis of the surface reconstruction of ultrathin alumina films.²

Over the course of the last 10 years, remarkable progress has been made on the determination of quasicrystal structure, notably on the fivefold Al-Pd-Mn surface.^{3–6} In 1994, a scanning tunneling microscopy experiment con-

ducted by Schaub *et al.*⁸ revealed fivefold motifs and a quaperiodic arrangement on the surface of the Al-Pd-Mn sample. Using dynamical low energy electron diffraction (LEED), Gierer *et al.*⁷ deduced on a bulk terminated fivefold Al-Pd-Mn surface with a density equal to 0.136 atoms/Å². Since then, intensive efforts have been put into the surface preparation of quasicrystals and atomically flat terraces have been formed routinely. As a consequence STM images of very high quality have been recorded, permitting for the first time a comparison between experimental observations in real space and bulk planes.^{9–13} This work has led to a better understanding of how to dissect bulk models in order to generate surface planes.^{12–14} In addition, by considering precise density rules one can now predict which planes should be stable at the surface of the fivefold Al-Pd-Mn sample.¹⁵

Progress in computational methods and the increasing power of the available computers now allows us to also obtain structural and electronic information from *ab initio* calculations on highly realistic structural models. The electron charge density distribution has been recently calculated in the *i*-Al-Pd-Mn model using advanced local-density functional techniques.¹⁶ The Vienna *ab initio* simulation package VASP has been used to perform *ab initio* electronic structure calculations and structural optimizations. Previously,^{10–12} it had been shown that the surface structure is best described in terms of a Penrose tiling (P1). This was supported by the *ab initio* calculation: the P1 tiling with vertices occupied by transition-metal atoms remains stable after relaxation. The surface charge density also showed flat minima at the centers of Bergman clusters and a strong charge depletion around the centers of some of the pseudo-Mackay clusters. These charge depletions suggest the existence of “surface vacancies” at the *i*-Al-Pd-Mn surface.

As mentioned above, STM experiments have played a major part in determining the surface structure of quasicrys-

tals through comparison of STM images with hard sphere models of surfaces. However, STM probes the electronic local density of state (LDOS) at the surface, and such comparisons are thus a first approximation. In this paper, we compare directly *ab initio* calculated STM images for a fivefold Al-Pd-Mn surface with experimental STM data. In Sec. II we describe briefly how the structural model used for the calculation is generated. Due to the thickness of the slab (357 atoms) selected no relaxation can be introduced and atoms remain at their ideal bulk positions. The atomic structure, the charge density distribution, the calculated STM images (constant height, constant current), and a comparison with experimental STM images are presented in Sec. III. Several characteristic features observed on experimental STM images are perfectly reproduced in the calculated STM images. These motifs structurally related to pseudo-Mackay and pseudo-Bergman clusters are also described along with the influence of the chemical element on the contrast in STM images. Finally, the origin of the fivefold surface vacancies are discussed in Sec. IV.

II. STRUCTURAL MODEL OF SURFACE OF *I*-Al-Pd-Mn

The starting point for the *ab initio* calculations is a structural model of the quasicrystalline surface of *i*-Al-Pd-Mn obtained from a model of the bulk quasicrystal. To describe the structure of *i*-Al-Pd-Mn, we have used the Katz-Gratias-Boudard (KGB) model.^{17–21} The KGB model of *i*-Al-Pd-Mn quasicrystal is defined in a six-dimensional (6D) hyperspace. The vertices of a six-dimensional face-centered-cubic lattice are decorated by three kinds of triacontahedral atomic surfaces. The atomic surfaces have an inner shell structure determining the chemical order of the quasicrystal. As the sizes of the shells are expressed as simple multiples of powers of the golden mean τ , it is easy to impose a linear phason strain and thus to construct well-defined periodic approximants. The KGB model agrees well with the experimental diffraction data, density, and stoichiometry.^{17,19,22,23} The stoichiometry of the KGB model, $\text{Al}_{0.7073}\text{Pd}_{0.2063}\text{Mn}_{0.0864}$, is in very good agreement with the experimentally determined composition of the icosahedral phase, $\text{Al}_{0.711}\text{Pd}_{0.202}\text{Mn}_{0.087}$ (Ref. 11) or $\text{Al}_{0.705}\text{Pd}_{0.21}\text{Mn}_{0.085}$ (Ref. 24). The KGB model also provides very good agreement of the calculated photoemission spectra with the experimental ones.²⁵

Our model of the quasicrystalline surface is obtained from the structure of an icosahedral approximant by cleaving at a plane perpendicular to one of the fivefold axes. The position of the cleavage plane is chosen such as to create a surface of high atomic density.¹⁵ Planes with high atomic density are separated by gaps of low atomic density. The gaps in the atomic density between high-density planes are natural cleavage planes of the quasicrystal.¹⁵ The distances between the planes with minimal atomic density form a Fibonacci-like sequence. One can recognize three different distances: $s=2.52$ Å, $m=4.08$ Å, and $l=s+m=6.60$ Å. The theoretical values of these distances were derived and reported by Papadopolos *et al.*¹² The sequence of the distances s , m , l corresponds to the sequence of terraces in the STM images mea-

sured by Schaub *et al.*⁸ and Shen *et al.*⁹ A quasicrystalline approximant can thus be decomposed into a sequence of slabs of three different thicknesses. According to their thickness s , m , and l we denote these slabs as S, M, and L, respectively. The S slab consists of three layers of atoms, the M slab consists of five, and the L slab of eight layers of atoms. A model of a quasicrystalline surface is created by cleaving the approximant at a plane separating the slabs. As a model of a fivefold surface of the Al-Pd-Mn quasicrystal we have chosen the surface of the M slab. This choice corresponds to one of the most frequently reported terminations of *i*-Al-Pd-Mn perpendicular to a fivefold axis.

The real-space structure of *i*-Al-Pd-Mn is often discussed in terms of pseudo-Mackay (M) and Bergman (B) clusters.²⁶ Each bc-site of the hypercubic 6D structure of *i*-Al-Pd-Mn is a center of a B cluster. The B cluster consists of 33 atoms with a Pd atom in the center. The M clusters are centered by Mn atoms. The first atomic shell surrounding Mn in the M cluster is very irregular. Seven or eight atoms occupy vertices of a small dodecahedron, but their spatial arrangement around the central Mn atom is irregular with respect to the icosahedral symmetry. The second shell consists of an icosahedron (12 atoms) and the third shell of an icosidodecahedron (30 atoms). The B and M clusters are mutually interpenetrating. An outer part of a B cluster is shared with an M cluster and vice versa. This overlap of the clusters leads to a conflict between their building principles and chemical decorations, eventually causing a substitutional defect or incompleteness of one of the clusters.

Our model of the quasicrystalline surface is the surface of the M slab cut from the $3/2$ -approximant. The structural model consists of 357 atoms. The surface measures 39.40 Å \times 32.86 Å and its thickness is 4.08 Å. This thickness of the slab is too small to support the surface during a relaxation by interatomic forces. The surface relaxation and its influence on the atomic positions and charge distributions have been investigated in our previous paper using a thicker slab cut from a lower-order $2/1$ approximant.¹⁶ From the study of the smaller $2/1$ approximant we have found that relaxation has only a modest influence on the structure of the surface, particularly it was shown that there is no surface reconstruction. In the present work we did not relax the surface, the atoms in the M slab remain at their ideal bulk positions. A larger, thicker model consisting of two slabs—the M slab and the adjacent S slab—would have 535 atoms. This size is already prohibitively large for the structural relaxation using *ab initio* calculations. The computational cell for the electronic structure calculations for the M slab cut from the $3/2$ approximant has an orthorhombic shape, and it includes a 6 Å wide vacuum layer.

III. RESULTS

The quasiperiodic ordering on the fivefold *i*-Al-Pd-Mn surface can be described by a planar P1 tiling.¹² At the surface one can recognize regular arrangements of atoms with pentagonal symmetry that correspond to the B and M clusters truncated by the cleavage plane. The centers of the B clusters are located in the central plane of the M slab. The

atomic structures of both surfaces of the M slab, front and rear, are thus almost identical. They differ only in some details related by symmetry operations.

Figure 1(a) shows the atomic structure of the surface of the 3/2-model derived from the KGB model of bulk *i*-Al-Pd-Mn. The surface is covered by a periodic approximant of a quasiperiodic P1 tiling. The edge of the P1 tiling measures 7.76 Å. The tiling in the figure consists of several different tiles—of a regular pentagon, a pentagonal star, a boat, and of thin and thick golden rhombuses. The P1 tiling is a planar tiling which can be obtained by projection from a 5D hyperspace. The acceptance domain (also termed the occupation domain or a window) of the P1 tiling is a decagon. The decagonal acceptance domains of the P1 tiling correspond to the maximal cross sections of the triacontahedral acceptance domains in 6D hyperspace defining the three-dimensional structure of the bulk quasicrystal.

The centers of the pentagonal tiles are chosen to correspond to the positions of the *M* clusters. In the P1 tiling the pentagonal tiles adopt two different orientations. The orientation of the pentagonal tiles is related to the vertical position of the Mn atoms centering the *M* clusters. According to this vertical position we designate the pentagonal tiles as “top” and “bottom.” In the top pentagon the center of the *M* cluster is at the top surface of the slab chosen to represent the surface. In the bottom pentagon the center of the *M* cluster is at a position deeper (2.56 Å) inside the slab (see Ref. 16 for more details). We note that any neighboring pentagons that share one edge have always opposite orientations.

Figure 1(a) demonstrates that most vertices of the P1 tiling coincide with the positions of the Pd atoms in the centers of the truncated *B* clusters from the midplane of the M slab. As the minimal distance between two *B* clusters is 7.76 Å not all vertices of the P1 tiling can be occupied by a *B* cluster. The pentagonal tiles are located at the positions of the *M* clusters centered by the Mn atoms. Another view on the surface is represented in Fig. 1(b) by the charge density distribution in the plane of the top atomic layer. The top layer is occupied only by Al atoms and a few ($\approx 2\%$) Mn atoms.^{6,7,15} The ideal surface consists of two closely spaced atomic layers separated by a vertical distance of only 0.48 Å. The Mn atom in the center of the pentagonal star is also located in this subsurface layer. The total surface atomic density of the model derived from the 3/2-approximant is $n_s = 0.132$ atoms/Å². This value is in very good agreement with the experimental value of 0.136 atoms/Å² reported by Gierer *et al.*⁷

The electron charge density distribution in the model of the *i*-Al-Pd-Mn quasicrystal has been calculated using advanced local-density-functional techniques. We have used the Vienna *ab initio* simulation package VASP.^{27,28} VASP performs an iterative diagonalization of the Kohn-Sham Hamiltonian. The calculations were performed within the generalized-gradient approximation (GGA).²⁹ The projector-augmented-wave version (PAW)²⁸ of VASP calculates the exact all-electron potentials eigenstates and charge densities, hence it produces very realistic valence-electron distributions.

Figure 1(b) shows the electron density in the surface layer. The figure shows that the Pd atoms from the next layer

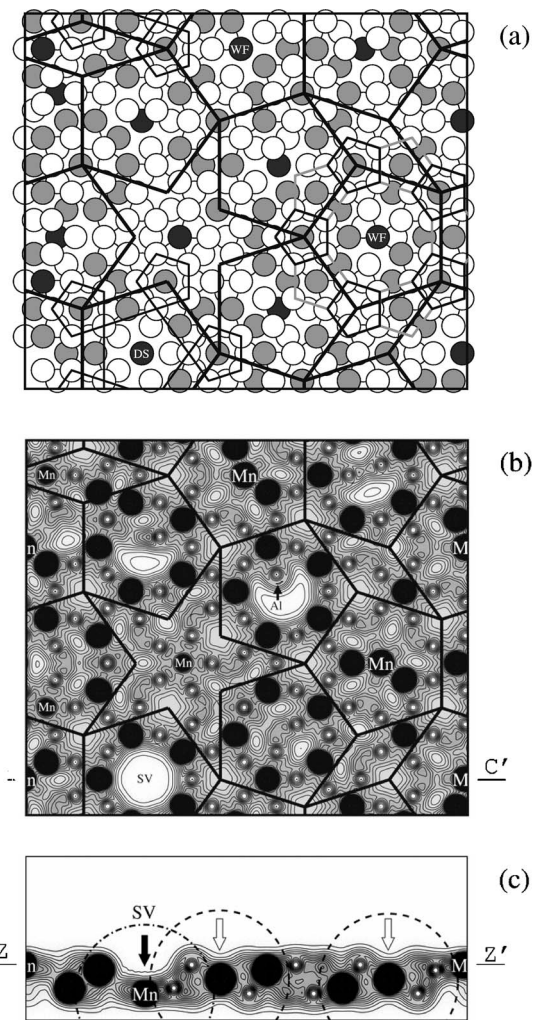


FIG. 1. The atomic structure of the fivefold surface of *i*-Al-Pd-Mn represented by the M slab cut from the 3/2 approximant. (a) The surface is covered by a part of a P1 tiling (thick lines), as described in the text. The positions of atoms are displayed by circles: Al—open circles, Pd—shaded circles, and Mn—closed circles. The pentagons drawn by thin lines represent skeletons of two characteristic features seen in STM images, a *white flower* (WF) and a *dark star* (DS), compare with Figs. 4 and 5. Part (b) shows the electronic charge density distribution of the same model. The contour plot presents the valence charge density distribution in a plane [marked Z-Z' in part (c)] intersecting the top atomic layer. The most striking features are the charge depletions inside some of the pentagonal tiles. They correspond to surface vacancies. Part (c) shows a section perpendicular to the surface displaying the valence charge density distribution at the position of the largest surface vacancy (SV). The contour plot represents a cut through the charge density distribution along a line joining the points CC' shown in (b). The section goes also through the centers of two *B* clusters. The *B* clusters are marked by dashed circles, *M* clusters by dot-dashed circles. The dark arrow indicates the position of the surface vacancy, the open arrows show the position of small charge depletions inside the centers of truncated *B* clusters.

located 0.48 Å below the top layer also contribute to the surface charge density. The charge density minima at the vertices of the P1 tiling occupied by Pd atoms are sur-

rounded by a complete or incomplete pentagon of Al atoms. The Pd atoms in the centers of the truncated *B* clusters are located deeper (1.26 Å) below the surface and their electrons do not contribute substantially to the surface charge density. The most striking features of the surface charge density distribution are large charge density minima inside some of the pentagonal tiles. These charge depletions correspond to surface vacancies. These vacancies are the consequence of the irregular structure of the first atomic shell surrounding the Mn atoms in the center of the *M* clusters. In a regular Mackay cluster the first atomic shell consists of 12 atoms forming a small icosahedron. In the *M* clusters in *i*-Al-Pd-Mn the central Mn atom has a lower coordination of 7 to 8 atoms,²¹ as confirmed by EXAFS experiments.³⁰ These atoms are distributed over the sites of a small dodecahedron, leaving other sites vacant such that their spatial arrangement breaks the local icosahedral symmetry. The vacancies exist also in the idealized structure. The existence of “vacancies” (or rather less dense regions) in the structure of bulk *i*-Al-Pd-Mn has been confirmed experimentally by Sato *et al.*³¹ The vacancies and their behavior under thermodynamic treatment have been studied experimentally by Ebert *et al.*³²

The shape of the surface vacancies depends on the position of atoms in the low-coordinated shell around the central Mn atom in the center of the *M* cluster. Some of the vacancies are large and exhibit fivefold symmetry. Such vacancies appear in the “bottom” pentagonal tiles only. The bottom of the vacancy is formed by the Mn atom surrounded by five atoms out of the 7 to 8 atoms forming the first low-coordinated shell. If the remaining 2 to 3 atoms are located deeper in the bulk, than the vacancy at the surface has the shape of a pentagonal hollow.

Figure 1(c) shows a section perpendicular to the surface displaying the valence charge density distribution at the position of the largest surface vacancy. The contour plot represents a cut through the charge density distribution in a plane perpendicular to the surface at the position of lines CC', see Fig. 1(b). The section goes also through the centers of two *B* clusters. The *B* clusters are marked by dashed circles, *M* clusters by dot-dashed circles. From the contour plot in Fig. 1(c) the depth of the surface vacancy can be estimated to be 2.2 Å while the depth of the charge density minima at the centers of the Bergman cluster is ≈ 0.7 Å only.

Figure 2 shows a simulated STM image of our 3/2 approximant calculated according to the Tersoff-Hamann approximation³³ from the surface charge density distribution. The calculation was performed for an STM image measured at a voltage +0.37 V. With this choice of the STM parameters, the tunneling current is dominated by electrons from unoccupied states up to 0.37 eV above the Fermi level. The STM image calculated for occupied states gives a similar result, albeit with a little lower contrast. Part (a) simulates an image taken at constant height of the tip 2.0 Å above the surface plane. The individual atoms are clearly recognized. Unfortunately, real measurements at such close distances are not feasible. Part (b) is a simulation corresponding to a STM image measured at constant current. This figure better corresponds to the experimental setup and more resembles the experimentally measured STM figures, see Fig. 3. However, the figure is more diffuse and information about the positions of individual atoms is not so clear.

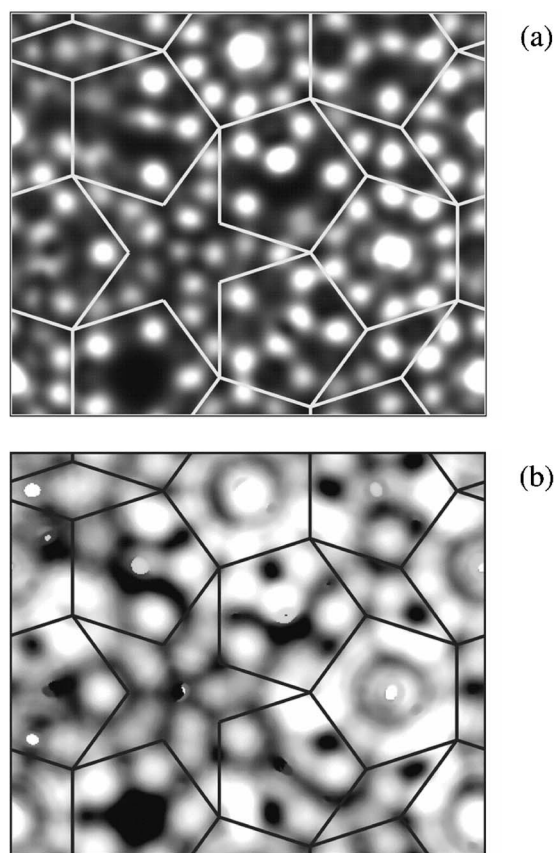


FIG. 2. STM images of the 3/2 approximant calculated from the surface charge density distribution. The calculation was performed for a STM image measured at voltage +0.37 V. This size and polarity of the voltage corresponds to contributions from unoccupied states up to 0.37 eV above the Fermi level. Part (a) simulates a measurement at constant height 2.0 Å above the surface plane. The individual atoms are clearly recognized. Part (b) simulates an STM image measured at constant current.

From the comparison of Fig. 2 with the structural model in Fig. 1 one can make the following observations.

(i) The STM image is dominated by the distribution of the Al atoms. They are seen as bright spots. On the other hand the Pd atoms are almost invisible in the STM image. They manifest themselves as dark spots. The STM image thus provides a quite different view of the surface compared to the charge density distribution shown in Fig. 1(b). The reason for the low contribution of the Pd atoms to the STM signal is primarily in the low density of Pd states in the vicinity of the Fermi level. Moreover, the Pd *d* states are more localized than the *s*, *p*-states of the Al atoms. Pd atoms are also deeper (by 0.48 Å) below the surface than the Al atoms.

In previous work we have found that the local paramagnetic density of states at the Fermi level on Mn atoms is extraordinarily large—up to nine states (eV atom)⁻¹. This value is three times larger than the highest value observed in Al-Mn compounds^{34,35} and up to 20 times higher than that on the Al atoms. The origin of the enhanced local DOS on the surface Mn atoms is just their low coordination as discussed above, leading to a very low width of the Mn *d* band. Despite the localized character of the Mn *d* states the Mn atoms thus

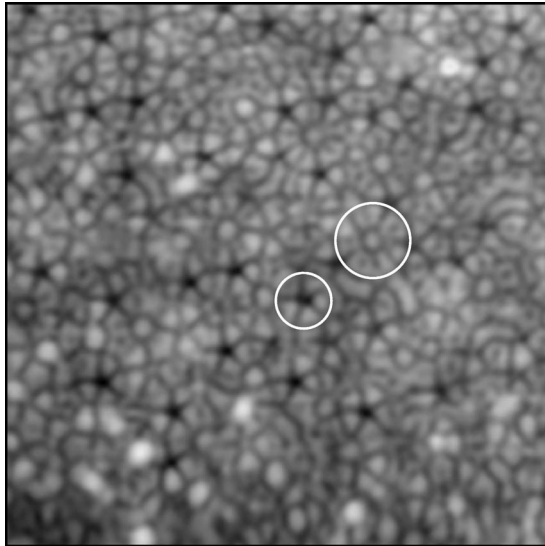


FIG. 3. $140 \text{ \AA} \times 140 \text{ \AA}$ high resolution STM image of fivefold *i*-Al-Pd-Mn ($I_t=0.14 \text{ nA}$, $V_b=+0.37 \text{ V}$). In the image the characteristic structural features—the *white flower* (WF) and the dark pentagonal hole, known as a *dark star* (DS), marked by larger and smaller circles, respectively—can be recognized.

can be well seen in the STM images as bright spots. In the present work we calculated the paramagnetic charge distribution only. However, it's worth remarking that the high DOS at E_F on Mn atoms can lead to a magnetic instability and the formation of a high localized magnetic moment. The d band is split into majority and minority bands. In this case the dominant contribution to the STM current comes from the part of the minority band overlapping with the energy interval 0.37 eV above the Fermi level. The magnetic splitting thus will reduce the STM signal. We assume that the extraordinarily bright spots in the experimental STM images correspond to paramagnetic Mn atoms, while the Mn atoms carrying magnetic moments would be seen as only moderately bright spots.

(ii) The Bergman clusters are seen in the STM image as pentagons with an edge of 2.96 \AA . However, from the comparison with Fig. 1(b) it is clear that not all such pentagons in the STM image correspond to Bergman clusters. The bright spots corresponding to the five Al atoms forming the pentagons are in most cases merged to one bigger spot. In the center of some of these spots one can observe a small dark spot. It is interesting that these small dark spots are darker if the Pd atom in the center of the pentagon is 0.48 \AA below the surface plane. In the case of Al pentagons corresponding to Bergman clusters where the central Pd atom is located at 1.26 \AA below the surface the spots are less dark.

(iii) In experimental STM images, (e.g., Fig. 3), one can recognize two characteristic features. The first one has been labeled the *white flower* (WF). The WF is formed by a central Mn atom surrounded by small Al pentagons with an edge measuring 2.96 \AA . These small Al pentagons form the “leaves” of the flower. Such configurations can be seen also in the experimental STM images of our model: they correspond to M clusters. For clarity in Fig. 4 one of these M clusters is shown separately and compared with its experi-

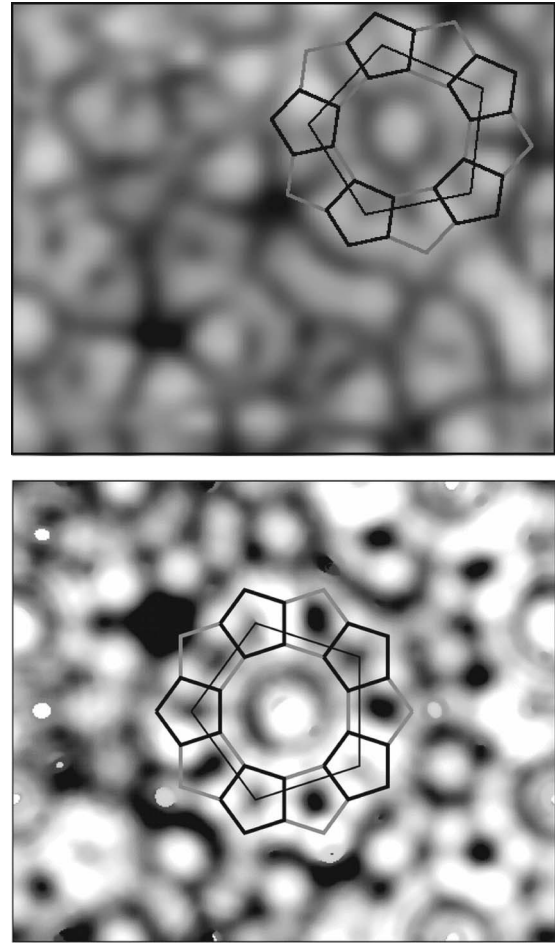


FIG. 4. A comparison of the experimental (top) and calculated (bottom) STM images of the *white flower* (WF). The area of the STM image ($39.5 \text{ \AA} \times 32.9 \text{ \AA}$) is the same as the size of the structural model. The WF corresponds to a M cluster (the central decagon) surrounded by five B clusters (black pentagons). The skeleton of the WF is formed by five dark and five gray pentagons of size 2.96 \AA , as described in the text, see also Fig. 1(a). The big pentagon marked by the thin line indicates the position of the “top” pentagonal tile of the P1 tiling.

mental image. WF's appear at the position of the “top” pentagonal tiles of the P1 tiling. In an ideal case the skeleton of the WF is formed by ten small pentagons surrounding the central Mn atom. Out of these ten small pentagons five belong to the B clusters centered in the vertices of the pentagonal P1 tile. They are marked in Fig. 4 by black lines. The other five pentagons, marked by gray lines, share four of their vertices with the neighboring black pentagons. Not all of the remaining vertices of the gray pentagons must be occupied by Al atoms. In Fig. 4 in one pentagon an Al atom is missing. However, if all vertices of the small gray pentagons are occupied, the skeleton of the WF has a tenfold symmetry. The atomic structure of a WF is presented also in Fig. 1(a). The centers of two WF's are there marked explicitly. The structure of a WF can be viewed in terms of individual atoms or in terms of clusters. From the viewpoint of its cluster structure a WF is formed by a central M cluster surrounded by five B clusters. The surface plane dissects the M cluster in

the center, at its equatorial position. The central Mn atom is thus exposed at the surface. While the first shells of the M cluster is irregular, the remaining shells are regular. Atoms of the third shell form an icosidodecahedron. This third shell is seen at the surface as a regular decagonal ring of Al atoms. Around each vertex of the top pentagonal tile there is a truncated B cluster manifesting itself at the surface as the small Al pentagon forming a leaf of the WF. Note that five intact B clusters “hanging down” from the surface can also form the “leaves” of the flower.¹²

(iv) The second well-known characteristic feature of the experimental STM images of the fivefold i -Al-Pd-Mn surfaces is the dark pentagonal hole. The most surprising result of the present comparison between the calculated and experimental STM images is a revised assignment of the origin of the dark pentagonal holes or “dark stars” (DS). So far it has been supposed^{16,36} that they correspond only to truncated Bergman (B) clusters. From the calculated STM image it is clear that they can originate from surface vacancies that exist inside some pseudo-Mackay (M) clusters. Figure 5 compares the calculated and experimental STM images of the dark pentagonal hole. From Figs. 1(a)–1(c) it is obvious that the DS is formed by a surface vacancy surrounded by a tenfold ring of atoms: a pentagon of Al atoms separated by 4.79 Å and a pentagon of Pd atoms of the same size. The contrast between the bright Al atoms and the dark Pd atoms forms the characteristic pentagonal “arms” of the DS in the STM image.

Both the WF and the DS characteristic patterns can appear in the STM images in a variety of different configurations. In our model the DS appears next to the WF. The distance between the centers of the WF and the DS is 10.73 Å. This is the distance between the centers of two adjacent pentagonal tiles with opposite orientation. The same configuration of WF and DS is frequently observed also in experimental STM images, see Fig. 3. In our calculated STM image in Fig. 2 one can also recognize an overlap of two WFs. The distance between their centers is 12.62 Å. It is the distance between the centers of two neighboring pentagonal tiles with the same orientations. Such a configuration is also observed in the experimental STM image presented in Fig. 3.

We note that the DS is not the only possible type of surface vacancy, however, it is the largest one. There can exist a smaller vacancy where the pentagonal hole DS is partially filled by an Al atom. Such a vacancy does not have the characteristic pentagonal shape. Of course, if the hole is filled by two Al atoms one cannot speak about vacancy anymore.

In the $3/2$ approximant only one surface vacancy in the form of DS is present. Although we have identified the clear physical origin of the atomic configuration that gives an STM contrast from this vacancy in the form of a DS, it is still possible to object that the atomic configuration could be an artifact of the $3/2$ approximant. A calculation of the STM image of a larger approximant is thus desirable. However, each next approximant contains $\tau^2 \approx 2.6$ times more atoms. A larger model of a surface based on the $5/3$ approximant consists of 930 atoms. This size is already too big for *ab initio* calculations. Nevertheless, on the basis of the information obtained from the $3/2$ approximant, particularly about the

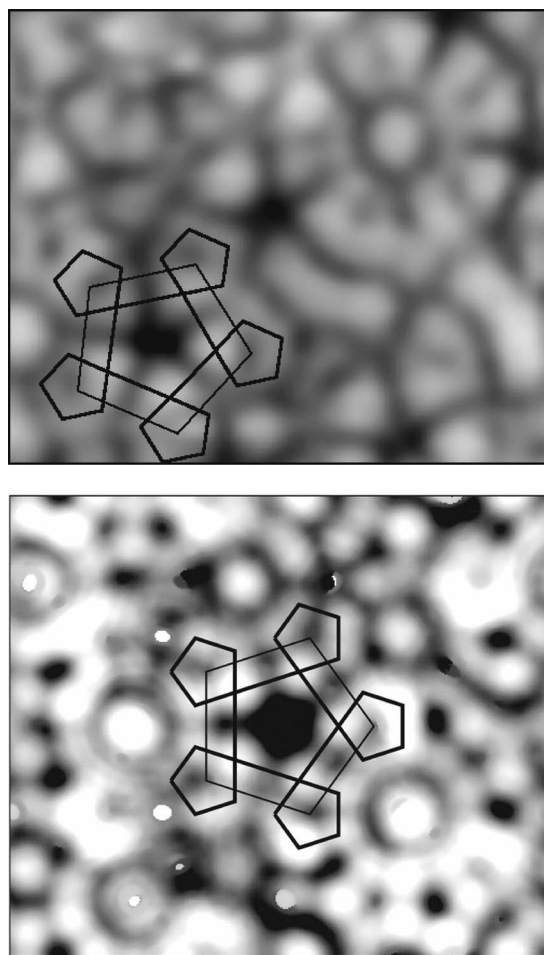


FIG. 5. A comparison of the experimental (top) and calculated (bottom) STM images of the dark pentagonal hole—*dark star* (DS). The area of the images is $39.5 \text{ \AA} \times 32.9 \text{ \AA}$. The DS is formed by a surface vacancy surrounded by a pentagon of Al atoms separated by 4.79 Å and a pentagon of Pd atoms of the same size forming in the STM image dark “arms” of the DS. The skeleton shown in the figure consists of one central pentagon of 4.79 Å surrounded by five pentagons of 2.96 Å, compare with Fig. 1(a). The big pentagon marked by the thin line indicates the position of the “bottom” pentagonal tile of the P1 tiling.

visibility of atoms in the STM image, one can calculate a simulated STM image also for larger approximants. The valence charge density distribution in the $5/3$ approximant has been approximated by parameterized analytic functions. The proper parameters have been chosen on the basis of the *ab initio* results. Figure 6 shows a structural model of the surface based on the $5/3$ approximant and its simulated STM image. One can recognize three surface vacancies in the form of the DS. As the size of the $5/3$ approximant is $62.5 \text{ \AA} \times 53.17 \text{ \AA}$ we can also estimate, the density of the DS vacancies as $\approx 0.9 \times 10^{-3} / \text{\AA}^2$. However, it has been shown that the density of DS varies with the surface terminations.^{14,36} The surface vacancies thus appear also in a larger model and seem to be an intrinsic property of the fivefold i -Al-Pd-Mn surface.

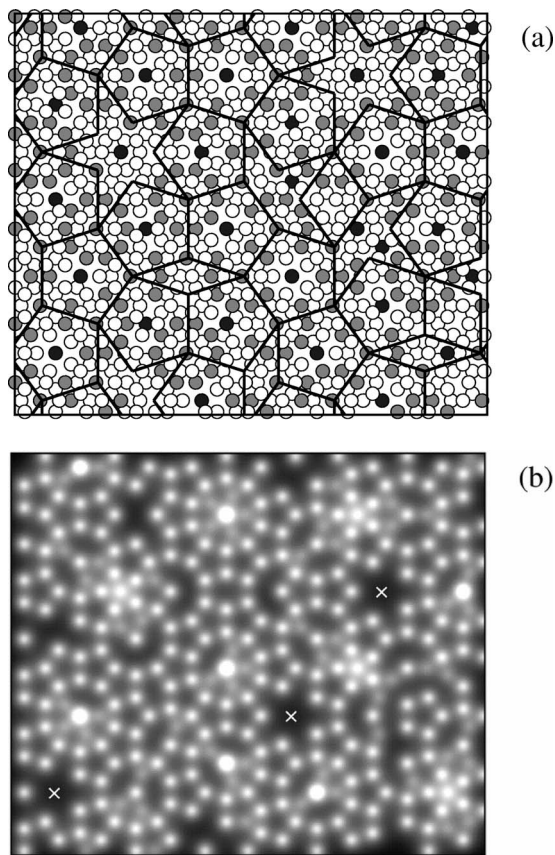


FIG. 6. A structural model of the *i*-Al-Pd-Mn surface based on the 5/3 approximant (a) and its simulated constant-height STM image (b). In part (a) the positions of atoms are displayed by circles: Al—open circles, Pd—shaded circles, and Mn—closed circles. In part (b) the positions of the DS's are marked by small white crosses.

IV. DISCUSSION AND CONCLUSIONS

The structure of the fivefold *i*-Al-Pd-Mn surface can be represented by the geometrical P1 tiling. Both characteristic features—the *whiteflower* and the *dark star*—seen in the STM images are related to the pentagonal tiles of the P1 tiling. The positions of the pentagonal tiles are chosen to coincide with the position of the truncated pseudo-Mackay (*M*) clusters. It is noteworthy that the position of the P1 tiling differs from previous work.^{10,12} There are two different orientations of the pentagonal tiles that we denote as “top” and “bottom.” In the top pentagons the central Mn atom of the *M* cluster is in the top atomic plane at the surface, and in the bottom pentagons the center of the *M* cluster is deeper beneath the surface plane. The WF is related to the top pentagons. It is formed by the central *M* cluster surrounded by five *B* clusters centered at the vertices of the pentagonal tile. The *B* clusters appear in the STM image as small Al pentagons with an edge measuring 2.96 Å. In the STM image the

bright spots corresponding to the individual Al atoms often merge into one larger bright spot, and the *B* clusters thus form the “leaves” of the WF. The DS is related to the bottom pentagons. It is also formed by the *M* cluster but centered 2.52 Å below the surface plane. The low-coordinated irregular first atomic shell of the *M* cluster manifests itself at the surface as a surface vacancy. The DS is formed by a surface vacancy surrounded by the tenfold ring of atoms—a pentagon of Al atoms with the edge measuring 4.79 Å and a pentagon of Pd atoms of the same size. The contrast between the bright Al atoms and the dark Pd atoms in the STM image forms the characteristic pentagonal shape of the DS. Because of the irregular arrangement of atoms in the first shell of the *M* cluster not all bottom pentagons appear at the surface as surface vacancies in the form of a DS. Some of them can be filled by one or two Al atoms.

It is important to note that the slab used here for the calculation is derived from the KGB model and is therefore not identical to the terminations presented by Papadopolos *et al.*¹² for the *M*-model.^{38–40} Whereas identical features are observed within both models, *B* clusters are not cut in the same way within the top surface layer. Prior to this *ab initio* calculation, the DS were thought to originate only from truncated *B* clusters¹² cut at a precise height (see Fig. 6 in Ref. 15). This conclusion was drawn by comparing experimental STM images with ball sphere models.¹² Within the model shown in Fig. 1(a) there is no *B* cluster dissected in this manner within the top surface layer. Hence DS were not expected within the calculated STM images shown in Fig. 5. However, surface vacancies clearly exhibit a DS pattern to that produced by truncated *B* clusters (4.08 Å from the top). Similar *ab initio* calculations on terminations presented by Papadopolos *et al.*¹² are now required to verify the presence of DS at the position of truncated *B* clusters.

It has been shown that *ab initio* calculated STM images resemble experimental STM images in very fine detail. The structure of the WF motifs is now understood as made of a truncated *M* cluster in the center with five *B* clusters as petals. The identification of the DS or dark pentagonal holes with the vacancies is another indication^{30–32,37} of the existence of such vacant, or more strictly speaking, less densely packed sites in the structure of the *i*-Al-Pd-Mn quasicrystals.

ACKNOWLEDGMENTS

This work has been supported by the Austrian Ministry for Education, Science and Art through the Center for Computational Materials Science. M.K. thanks also for support the Grant Agency for Science of Slovakia (No. 2/5096/25) and the Agency for Support of Science and Technology (Grants No. APVT-51021102, APVT-51052702, SO-51/03R80603). We also acknowledge support from the UK Engineering and Physical Sciences Research Council (GR/S19080/01).

- ¹A. Yamamoto, H. Takakura, and A. P. Tsai, *Phys. Rev. B* **68**, 094201 (2003).
- ²G. Kresse, M. Schmid, E. Napetschnig, M. Shishkin, L. Khler, and P. Varga, *Science* **308**, 1440 (2005).
- ³P. Ebert, M. Feuerbacher, N. Tamura, M. Wollgarten, and K. Urban, *Phys. Rev. Lett.* **77**, 3827 (1996).
- ⁴B. Bolliger, M. Erbudak, D. D. Vvedensky, M. Zurkirch, and A. R. Kortan, *Phys. Rev. Lett.* **80**, 5369 (1998).
- ⁵D. Naumović, P. Aebi, C. Beeli, and L. Schlapbach, *Surf. Sci.* **433–435**, 302 (1999).
- ⁶J. C. Zheng, C. H. A. Huan, A. T. S. Wee, M. A. Van Hove, C. S. Fadley, F. J. Shi, E. Rotenberg, S. R. Barman, J. J. Paggel, K. Horn, P. Ebert, and K. Urban, *Phys. Rev. B* **69**, 134107 (2004).
- ⁷M. Gierer, M. A. Van Hove, A. I. Goldman, Z. Shen, S.-L. Chang, P. J. Pinhero, C. J. Jenks, J. W. Andereg, C.-M. Zhang, and P. A. Thiel, *Phys. Rev. B* **57**, 7628 (1998).
- ⁸T. M. Schaub, D. E. Bürgler, H.-J. Güntherodt, and J.-B. Suck, *Phys. Rev. Lett.* **73**, 1255 (1994).
- ⁹Z. Shen, C. R. Stoldt, C. J. Jenks, T. A. Lograsso, and P. A. Thiel, *Phys. Rev. B* **60**, 14688 (1999).
- ¹⁰J. Ledieu, R. McGrath, R. D. Diehl, T. A. Lograsso, A. R. Ross, Z. Papadopolos, and G. Kasner, *Surf. Sci. Lett.* **492**, L729 (2001).
- ¹¹L. Barbier, D. Le Floc'h, Y. Calvayrac, and D. Gratias, *Phys. Rev. Lett.* **88**, 085506 (2002).
- ¹²Z. Papadopolos, G. Kasner, J. Ledieu, E. J. Cox, N. V. Richardson, Q. Chen, R. D. Diehl, T. A. Lograsso, A. R. Ross, and R. McGrath, *Phys. Rev. B* **66**, 184207 (2002).
- ¹³H. R. Sharma, V. Fournée, M. Shimoda, A. R. Ross, T. A. Lograsso, A. P. Tsai, and A. Yamamoto, *Phys. Rev. Lett.* **93**, 165502 (2004).
- ¹⁴G. Kasner, Z. Papadopolos, P. Kramer, and D. E. Bürgler, *Phys. Rev. B* **60**, 3899 (1999).
- ¹⁵Z. Papadopolos, P. Pleasants, G. Kasner, V. Fournée, C. J. Jenks, J. Ledieu, and R. McGrath, *Phys. Rev. B* **69**, 224201 (2004).
- ¹⁶M. Krajčí and J. Hafner, *Phys. Rev. B* **71**, 054202 (2005).
- ¹⁷M. Cornier-Quiquandon, A. Quivy, S. Lefebvre, E. Elkaim, G. Heger, A. Katz, and D. Gratias, *Phys. Rev. B* **44**, 2071 (1991).
- ¹⁸A. Katz and D. Gratias, *J. Non-Cryst. Solids* **153–154**, 187 (1993).
- ¹⁹M. Boudard, M. de Boissieu, C. Janot, G. Heger, C. Beeli, H.-U. Nissen, H. Vincent, R. Ibberson, M. Audier, and J. M. Dubois, *J. Phys.: Condens. Matter* **4**, 10149 (1992).
- ²⁰M. de Boissieu, P. Stephens, M. Boudard, C. Janot, D. L. Chapman, and M. Audier, *J. Phys.: Condens. Matter* **6**, 10725 (1994).
- ²¹M. Krajčí, M. Windisch, J. Hafner, G. Kresse, and M. Mihalkovič, *Phys. Rev. B* **51**, 17355 (1995).
- ²²E. Cockayne, R. Phillips, X. B. Kan, S. C. Moss, J. L. Robertson, T. Ishimasa, and M. Mori, *J. Non-Cryst. Solids* **153–154**, 140 (1993).
- ²³C. R. Lin, S. T. Lin, C. R. Wang, S. L. Chou, H. E. Horng, J. M. Cheng, Y. D. Yao, and S. C. Lai, *J. Phys.: Condens. Matter* **9**, 1509 (1997).
- ²⁴J. Delahaye, J. P. Brison, and C. Berger, *Phys. Rev. Lett.* **81**, 4204 (1998).
- ²⁵G. W. Zhang and Z. M. Stadnik, in *Proceedings of the 5th International Conference on Quasicrystals*, edited by C. Janot and R. Mosseri (World Scientific, Singapore, 1995), pp. 552–555.
- ²⁶D. Gratias, F. Puyraimond, M. Quiquandon, and A. Katz, *Phys. Rev. B* **63**, 024202 (2000).
- ²⁷G. Kresse and J. Furthmüller, *Comput. Mater. Sci.* **6**, 15 (1996); *Phys. Rev. B* **54**, 11169 (1996).
- ²⁸G. Kresse and D. Joubert, *Phys. Rev. B* **59**, 1758 (1999).
- ²⁹J. P. Perdew and Y. Wang, *Phys. Rev. B* **45**, 13244 (1992).
- ³⁰A. Sadoc and J. M. Dubois, *J. Non-Cryst. Solids* **153–154**, 83 (1993); *Philos. Mag. B* **66**, 541 (1992).
- ³¹K. Sato, Y. Takahashi, H. Uchiyama, I. Kanazawa, R. Tamura, K. Kimura, F. Komori, R. Suzuki, T. Ohdaira, and S. Takeuchi, *Phys. Rev. B* **59**, 6712 (1999).
- ³²P. Ebert, M. Yurechko, F. Kluge, T. Cai, B. Grushko, P. A. Thiel, and K. Urban, *Phys. Rev. B* **67**, 024208 (2003).
- ³³J. Tersoff and D. R. Hamann, *Phys. Rev. B* **31**, 805 (1985).
- ³⁴J. Hafner and M. Krajčí, *Phys. Rev. B* **57**, 2849 (1998).
- ³⁵M. Krajčí and J. Hafner, *Phys. Rev. B* **58**, 14110 (1998).
- ³⁶J. Ledieu and R. McGrath, *J. Phys.: Condens. Matter* **15**, S3113 (2003).
- ³⁷S. Lyonard, G. Coddens, Y. Calvayrac, and D. Gratias, *Phys. Rev. B* **53**, 3150 (1996).
- ³⁸V. Elser, *Philos. Mag. B* **73**, 641 (1996).
- ³⁹Z. Papadopolos, P. Kramer, and W. Liebermeister, in *Proceedings of the International Conference on Aperiodic Crystals*, edited by M. de Boissieu, J.-L. Verger-Gaugry, and R. Currat (World Scientific, Singapore, 1997), pp. 173–181.
- ⁴⁰P. Kramer, Z. Papadopolos, and W. Liebermeister, in *Proceedings of the 6th International Conference on Quasicrystals*, edited by S. Takeuchi and T. Fujiwara (World Scientific, Singapore, 1998), pp. 71–76.